PFU, plaque-forming unit; IRES, internal ribosome entry site; FITC, fluorescent isothiocyanate; MFI, mean fluorescence intensity.

CONFLICT OF INTEREST

Y Urata is an employee of Oncolys BioPharma, Inc., the manufacturer of OBP-401 (Telomescan). The remaining authors declare no conflict of interest.

ACKNOWLEDGEMENTS

We thank Dr Satoru Kyo (Kanazawa University) for providing the OST cells; Dr Hiroyuki Kawashima (Niigata University) for providing the NOS-10 and NMFH-1 cells; and Tomoko Sueishi for her excellent technical support. This study was supported by grants-in-Aid from the Ministry of Education, Science and Culture, Japan and grants from the Ministry of Health and Welfare, Japan.

REFERENCES

1 Kanerva A, Hemminki A. Adenoviruses for treatment of cancer. *Ann Med* 2005; **37**: 33-43.
2 Rein DT, Breidenbach M, Curiel DT. Current developments in adenovirus-based cancer gene therapy. *Future Oncol* 2006; **2**: 137-143.
3 Yamamoto M, Curiel DT. Current issues and future directions of oncolytic adenoviruses. *Mol Ther* 2010; **18**: 243-250.
4 Clayman GL, el-Naggar AK, Lippman SM, Henderson YC, Frederick M, Merritt JA *et al.* Adenovirus-mediated p53 gene transfer in patients with advanced recurrent head and neck squamous cell carcinoma. *J Clin Oncol* 1998; **16**: 2221-2232.
5 Swisher SG, Roth JA, Nemunaitis J, Lawrence DD, Kemp BL, Carrasco CH *et al.* Adenovirus-mediated p53 gene transfer in advanced non-small-cell lung cancer. *J Natl Cancer Inst* 1999; **91**: 763-771.
6 Shimada H, Matsubara H, Shiratori T, Shimizu T, Miyazaki S, Okazumi S *et al.* Phase I/II adenoviral p53 gene therapy for chemoradiation resistant advanced esophageal squamous cell carcinoma. *Cancer Sci* 2006; **97**: 554-561.
7 Fujiwara T, Tanaka N, Kanazawa S, Ohtani S, Saijo Y, Nukiwa T *et al.* Multicenter phase I study of repeated intratumoral delivery of adenoviral p53 in patients with advanced non-small-cell lung cancer. *J Clin Oncol* 2006; **24**: 1689-1699.
8 Fujiwara T, Urata Y, Tanaka N. Telomerase-specific oncolytic virotherapy for human cancer with the hTERT promoter. *Curr Cancer Drug Targets* 2007; **7**: 191-201.
9 Pesonen S, Kangasniemi L, Hemminki A. Oncolytic adenoviruses for the treatment of human cancer: focus on translational and clinical data. *Mol Pharm* 2011; **8**: 12-28.
10 Bergelson JM, Cunningham JA, Droguett G, Kurt-Jones EA, Krithivas A, Hong JS *et al.* Isolation of a common receptor for Coxsackie B viruses and adenoviruses 2 and 5. *Science* 1997; **275**: 1320-1323.
11 Hemmi S, Geertsen R, Mezzacasa A, Peter I, Dummer R. The presence of human coxsackievirus and adenovirus receptor is associated with efficient adenovirus-mediated transgene expression in human melanoma cell cultures. *Hum Gene Ther* 1998; **9**: 2363-2373.
12 Hutchin ME, Pickles RJ, Yarbrough WG. Efficiency of adenovirus-mediated gene transfer to oropharyngeal epithelial cells correlates with cellular differentiation and human coxsackie and adenovirus receptor expression. *Hum Gene Ther* 2000; **11**: 2365-2375.
13 You Z, Fischer DC, Tong X, Hasenburg A, Aguilar-Cordova E, Kieback DG. Coxsackievirus-adenovirus receptor expression in ovarian cancer cell lines is associated with increased adenovirus transduction efficiency and transgene expression. *Cancer Gene Ther* 2001; **8**: 168-175.
14 Rauen KA, Sudilovsky D, Le JL, Chew KL, Hann B, Weinberg V *et al.* Expression of the coxsackie adenovirus receptor in normal prostate and in primary and metastatic prostate carcinoma: potential relevance to gene therapy. *Cancer Res* 2002; **62**: 3812-3818.
15 Kim M, Zinn KR, Barnett BG, Sumerel LA, Krasnykh V, Curiel DT *et al.* The therapeutic efficacy of adenoviral vectors for cancer gene therapy is limited by a low level of primary adenovirus receptors on tumour cells. *Eur J Cancer* 2002; **38**: 1917-1926.
16 Qin M, Chen S, Yu T, Escuadro B, Sharma S, Batra RK. Coxsackievirus adenovirus receptor expression predicts the efficiency of adenoviral gene transfer into non-small cell lung cancer xenografts. *Clin Cancer Res* 2003; **9**: 4992-4999.
17 Douglas JT, Kim M, Sumerel LA, Carey DE, Curiel DT. Efficient oncolysis by a replicating adenovirus (ad) *in vivo* is critically dependent on tumor expression of primary ad receptors. *Cancer Res* 2001; **61**: 813-817.
18 Fuxe J, Liu L, Malin S, Philipson L, Collins VP, Pettersson RF. Expression of the coxsackie and adenovirus receptor in human astrocytic tumors and xenografts. *Int J Cancer* 2003; **103**: 723-729.
19 Marsee DK, Vadysirisack DD, Morrison CD, Prasad ML, Eng C, Duh QY *et al.* Variable expression of coxsackie-adenovirus receptor in thyroid tumors: implications for adenoviral gene therapy. *Thyroid* 2005; **15**: 977-987.
20 Anders M, Rosch T, Kuster K, Becker I, Hofler H, Stein HJ *et al.* Expression and function of the coxsackie and adenovirus receptor in Barrett's esophagus and associated neoplasia. *Cancer Gene Ther* 2009; **16**: 508-515.
21 Korn WM, Macal M, Christian C, Lacher MD, McMillan A, Rauen KA *et al.* Expression of the coxsackievirus- and adenovirus receptor in gastrointestinal cancer correlates with tumor differentiation. *Cancer Gene Ther* 2006; **13**: 792-797.
22 Gu W, Ogose A, Kawashima H, Ito M, Ito T, Matsuba A *et al.* High-level expression of the coxsackievirus and adenovirus receptor messenger RNA in osteosarcoma, Ewing's sarcoma, and benign neurogenic tumors among musculoskeletal tumors. *Clin Cancer Res* 2004; **10**: 3831-3838.
23 Kawashima H, Ogose A, Yoshizawa T, Kuwano R, Hotta Y, Hotta T *et al.* Expression of the coxsackievirus and adenovirus receptor in musculoskeletal tumors and mesenchymal tissues: efficacy of adenoviral gene therapy for osteosarcoma. *Cancer Sci* 2003; **94**: 70-75.
24 Rice AM, Currier MA, Adams LC, Bharatan NS, Collins MH, Snyder JD *et al.* Ewing sarcoma family of tumors express adenovirus receptors and are susceptible to adenovirus-mediated oncolysis. *J Pediatr Hematol Oncol* 2002; **24**: 527-533.
25 Matsumoto K, Shariat SF, Ayala GE, Rauen KA, Lerner SP. Loss of coxsackie and adenovirus receptor expression is associated with features of aggressive bladder cancer. *Urology* 2005; **66**: 441-446.
26 Anders M, Vieth M, Rocken C, Ebert M, Pross M, Gretschel S *et al.* Loss of the coxsackie and adenovirus receptor contributes to gastric cancer progression. *Br J Cancer* 2009; **100**: 352-359.
27 Yamamoto S, Yoshida Y, Aoyagi M, Ohno K, Hirakawa K, Hamada H. Reduced transduction efficiency of adenoviral vectors expressing human p53 gene by repeated transduction into glioma cells *in vitro*. *Clin Cancer Res* 2002; **8**: 913-921.
28 Tango Y, Taki M, Shirakiya Y, Ohtani S, Tokunaga N, Tsunemitsu Y *et al.* Late resistance to adenoviral p53-mediated apoptosis caused by decreased expression of Coxsackie-adenovirus receptors in human lung cancer cells. *Cancer Sci* 2004; **95**: 459-463.
29 Sasaki T, Tazawa H, Hasei J, Kunisada T, Yoshida A, Hashimoto Y *et al.* Preclinical evaluation of telomerase-specific oncolytic virotherapy for human bone and soft tissue sarcomas. *Clin Cancer Res* 2011; **17**: 1828-1838.
30 Kawashima T, Kagawa S, Kobayashi N, Shirakiya Y, Umeoka T, Teraishi F *et al.* Telomerase-specific replication-selective virotherapy for human cancer. *Clin Cancer Res* 2004; **10** (1 Pt 1): 285-292.
31 Hashimoto Y, Watanabe Y, Shirakiya Y, Uno F, Kagawa S, Kawamura H *et al.* Establishment of biological and pharmacokinetic assays of telomerase-specific replication-selective adenovirus. *Cancer Sci* 2008; **99**: 385-390.
32 Kishimoto H, Kojima T, Watanabe Y, Kagawa S, Fujiwara T, Uno F *et al. In vivo* imaging of lymph node metastasis with telomerase-specific replication-selective adenovirus. *Nat Med* 2006; **12**: 1213-1219.
33 Kishimoto H, Urata Y, Tanaka N, Fujiwara T, Hoffman RM. Selective metastatic tumor labeling with green fluorescent protein and killing by systemic administration of telomerase-dependent adenoviruses. *Mol Cancer Ther* 2009; **8**: 3001-3008.
34 Kojima T, Hashimoto Y, Watanabe Y, Kagawa S, Uno F, Kuroda S *et al.* A simple biological imaging system for detecting viable human circulating tumor cells. *J Clin Invest* 2009; **119**: 3172-3181.
35 Kishimoto H, Zhao M, Hayashi K, Urata Y, Tanaka N, Fujiwara T *et al. In vivo* internal tumor illumination by telomerase-dependent adenoviral GFP for precise surgical navigation. *Proc Natl Acad Sci USA* 2009; **106**: 14514-14517.
36 Feero WG, Rosenblatt JD, Huard J, Watkins SC, Epperly M, Clemens PR *et al.* Viral gene delivery to skeletal muscle: insights on maturation-dependent loss of fiber infectivity for adenovirus and herpes simplex type 1 viral vectors. *Hum Gene Ther* 1997; **8**: 371-380.
37 Hoffman RM. The multiple uses of fluorescent proteins to visualize cancer *in vivo*. *Nat Rev Cancer* 2005; **5**: 796-806.
38 Hoffman RM, Yang M. Subcellular imaging in the live mouse. *Nat Protoc* 2006; **1**: 775-782.
39 Shay JW, Bacchetti S. A survey of telomerase activity in human cancer. *Eur J Cancer* 1997; **33**: 787-791.
40 Marsman WA, Buskens CJ, Wesseling JG, Offerhaus GJ, Bergman JJ, Tytgat GN *et al.* Gene therapy for esophageal carcinoma: the use of an explant model to test adenoviral vectors *ex vivo*. *Cancer Gene Ther* 2004; **11**: 289-296.
41 Wang Y, Thorne S, Hannock J, Francis J, Au T, Reid T *et al.* A novel assay to assess primary human cancer infectibility by replication-selective oncolytic adenoviruses. *Clin Cancer Res* 2005; **11**: 351-360.
42 Zeimet AG, Muller-Holzner E, Schuler A, Hartung G, Berger J, Hermann M *et al.* Determination of molecules regulating gene delivery using adenoviral vectors in ovarian carcinomas. *Gene Therapy* 2002; **9**: 1093-1100.
43 Kuster K, Koschel A, Rohwer N, Fischer A, Wiedenmann B, Anders M. Downregulation of the coxsackie and adenovirus receptor in cancer cells by hypoxia depends on HIF-1alpha. *Cancer Gene Ther* 2010; **17**: 141-146.

© 2013 Macmillan Publishers Limited

44 Seidman MA, Hogan SM, Wendland RL, Worgall S, Crystal RG, Leopold PL. Variation in adenovirus receptor expression and adenovirus vector-mediated transgene expression at defined stages of the cell cycle. *Mol Ther* 2001; **4**: 13–21.
45 Hotta T, Motoyama T, Watanabe H. Three human osteosarcoma cell lines exhibiting different phenotypic expressions. *Acta Pathol Jpn* 1992; **42**: 595–603.
46 Kawashima H, Ogose A, Gu W, Nishio J, Kudo N, Kondo N *et al.* Establishment and characterization of a novel myxofibrosarcoma cell line. *Cancer Genet Cytogenet* 2005; **161**: 28–35.
47 Kunisada T, Miyazaki M, Mihara K, Gao C, Kawai A, Inoue H *et al.* A new human chondrosarcoma cell line (OUMS-27) that maintains chondrocytic differentiation. *Int J Cancer* 1998; **77**: 854–859.

Supplementary Information accompanies the paper on Gene Therapy website (http://www.nature.com/gt)

© 2013 Macmillan Publishers Limited

Molecular Cancer Therapeutics

Dual Programmed Cell Death Pathways Induced by p53 Transactivation Overcome Resistance to Oncolytic Adenovirus in Human Osteosarcoma Cells

Joe Hasei[1], Tsuyoshi Sasaki[1], Hiroshi Tazawa[2,4], Shuhei Osaki[1], Yasuaki Yamakawa[1], Toshiyuki Kunisada[1,3], Aki Yoshida[1], Yuuri Hashimoto[2], Teppei Onishi[2], Futoshi Uno[2], Shunsuke Kagawa[2], Yasuo Urata[5], Toshifumi Ozaki[1], and Toshiyoshi Fujiwara[2]

Abstract

Tumor suppressor p53 is a multifunctional transcription factor that regulates diverse cell fates, including apoptosis and autophagy in tumor biology. p53 overexpression enhances the antitumor activity of oncolytic adenoviruses; however, the molecular mechanism of this occurrence remains unclear. We previously developed a tumor-specific replication-competent oncolytic adenovirus, OBP-301, that kills human osteosarcoma cells, but some human osteosarcoma cells were OBP-301–resistant. In this study, we investigated the antitumor activity of a p53-expressing oncolytic adenovirus, OBP-702, and the molecular mechanism of the p53-mediated cell death pathway in OBP-301–resistant human osteosarcoma cells. The cytopathic activity of OBP-702 was examined in OBP-301–sensitive (U2OS and HOS) and OBP-301–resistant (SaOS-2 and MNNG/HOS) human osteosarcoma cells. The molecular mechanism in the OBP-702–mediated induction of two cell death pathways, apoptosis and autophagy, was investigated in OBP-301–resistant osteosarcoma cells. The antitumor effect of OBP-702 was further assessed using an orthotopic OBP-301–resistant MNNG/HOS osteosarcoma xenograft tumor model. OBP-702 suppressed the viability of OBP-301–sensitive and -resistant osteosarcoma cells more efficiently than OBP-301 or a replication-deficient p53-expressing adenovirus (Ad-p53). OBP-702 induced more profound apoptosis and autophagy when compared with OBP-301 or Ad-p53. E1A-mediated *miR-93/106b* upregulation induced p21 suppression, leading to p53-mediated apoptosis and autophagy in OBP-702–infected cells. p53 overexpression enhanced adenovirus-mediated autophagy through activation of damage-regulated autophagy modulator (DRAM). Moreover, OBP-702 suppressed tumor growth in an orthotopic OBP-301–resistant MNNG/HOS xenograft tumor model. These results suggest that OBP-702–mediated p53 transactivation is a promising antitumor strategy to induce dual apoptotic and autophagic cell death pathways via regulation of miRNA and DRAM in human osteosarcoma cells. *Mol Cancer Ther; 12(3); 314–25. ©2012 AACR.*

Introduction

Osteosarcoma is one of the most common malignant tumors in young children (1, 2). Current treatment strategies, which consist of multi-agent chemotherapy and aggressive surgery, have significantly improved the cure rate and prognosis of patients with osteosarcoma. In fact, over the past 30 years, the 5-year survival rate has increased from 10% to 70% (3–5). Even in patients with osteosarcoma with metastases at diagnosis, the 5-year survival rate has reached 20% to 30% in response to chemotherapy and surgical removal of primary and metastatic tumors (6). However, treatment outcomes for patients with osteosarcomas have further improved over the last few years. Therefore, the development of novel therapeutic strategies is required to improve the clinical outcomes in patients with osteosarcomas.

Tumor-specific replication-competent oncolytic viruses are being developed as novel anticancer therapy, in which the promoters of cancer-related genes are used to regulate virus replication in a tumor-dependent manner. More than 85% of all human cancers express high telomerase activity to maintain the length of the telomeres during cell division, whereas normal somatic cells seldom show this enhanced telomerase activity (7, 8). Telomerase activity has also been detected in 44% to 81% of bone and

Authors' Affiliations: Departments of [1]Orthopaedic Surgery, [2]Gastroenterological Surgery, and [3]Medical Materials for Musculoskeletal Reconstruction, Okayama University Graduate School of Medicine, Dentistry and Pharmaceutical Sciences; [4]Center for Innovative Clinical Medicine, Okayama University Hospital, Okayama; and [5]Oncolys BioPharma, Inc., Tokyo, Japan

Note: Supplementary data for this article are available at Molecular Cancer Therapeutics Online (http://mct.aacrjournals.org/).

Corresponding Author: Toshiyoshi Fujiwara, Department of Gastroenterological Surgery, Okayama University Graduate School of Medicine, Dentistry and Pharmaceutical Sciences, 2-5-1 Shikata-cho, Kita-ku, Okayama 700-8558, Japan. Phone: 81-86-235-7257; Fax: 81-86-221-8775; E-mail: toshi_f@md.okayama-u.ac.jp

doi: 10.1158/1535-7163.MCT-12-0869

©2012 American Association for Cancer Research.

soft-tissue sarcomas (9, 10). Telomerase activation is closely correlated with the expression of the human telomerase reverse transcriptase (*hTERT*) gene (11). On the basis of these data, we previously developed a telomerase-specific replication-competent oncolytic adenovirus OBP-301 (Telomelysin) in which the *hTERT* gene promoter drives the expression of the *E1A* and *E1B* genes (12). A phase I clinical trial of OBP-301, which was conducted in the United States on patients with advanced solid tumors, indicated that OBP-301 was well tolerated by patients (13). Recently, we reported that OBP-301 efficiently killed human bone and soft-tissue sarcoma cells (14, 15). However, some osteosarcoma cell lines were not sensitive to the antitumor effect of OBP-301. Therefore, to efficiently eliminate tumor cells with OBP-301, its antitumor effects need to be enhanced.

Cancer gene therapy is defined as the treatment of malignant tumors via the introduction of a therapeutic tumor suppressor gene or the abrogation of an oncogene. The tumor suppressor *p53* gene has an attractive tumor suppressor profile as a potent therapeutic transgene for induction of cell-cycle arrest, senescence, apoptosis, and autophagy (16). Dual cell death pathways, such as apoptosis and autophagy, induced by p53 transactivation are mainly involved in the suppression of tumor initiation and progression. However, among the p53 downstream target genes, p21, which is most rapidly and strongly induced during the DNA damage response, mainly induces cell-cycle arrest through suppression of apoptotic and autophagic cell death pathways (17, 18). Thus, p21 suppression may be a more effective strategy for the induction of apoptotic and autophagic cell death pathways in tumor cells, particularly when the tumor suppressor *p53* gene is overexpressed in tumor cells in response to cancer gene therapy.

A p53-expressing replication-deficient adenovirus (Ad-p53, Advexin) has previously been reported to induce an antitumor effect in the *in vitro* and *in vivo* settings (19, 20) as well as in some clinical studies (21–24). We recently reported that combination therapy with OBP-301 and Ad-p53 resulted in a more profound antitumor effect than monotherapy with either OBP-301 or Ad-p53 (25). Moreover, we generated armed OBP-301 expressing the wild-type *p53* tumor suppressor gene (OBP-702) and showed that OBP-702 suppressed the viability of various types of epithelial malignant cells more efficiently than did OBP-301 (26). OBP-702 induced a more profound apoptotic cell death effect than Ad-p53, likely via adenoviral E1A-mediated suppression of anti-apoptotic p21 in human epithelial malignant cells. However, it remained unclear whether OBP-702 efficiently induces an antitumor effect in human nonepithelial malignant cells, including osteosarcomas.

In the present study, we investigated the *in vitro* cytopathic efficacy of the p53-expressing telomerase-specific replication-competent oncolytic adenovirus, OBP-702, in human osteosarcoma cells, and we compared the induction level of apoptotic and autophagic cell deaths in OBP-301–resistant human osteosarcoma cells infected with OBP-301, OBP-702, and Ad-p53. The molecular mechanism by which OBP-702 mediates induction of apoptosis and autophagy was also investigated. Finally, the *in vivo* antitumor effect of OBP-702 was evaluated using an orthotopic OBP-301–resistant human osteosarcoma xenograft tumor model.

Materials and Methods

Cell lines

The human osteosarcoma cell lines, HOS and SaOS-2, were kindly provided by Dr. Satoru Kyo (Kanazawa University, Ishikawa, Japan). These cells were propagated as monolayer cultures in Dulbecco's Modified Eagle's Medium. The human osteosarcoma cell line, U2OS, was obtained from the American Type Culture Collection and was grown in McCoy's 5a Medium. The human osteosarcoma cell line, MNNG/HOS, was purchased from DS Pharma Biomedical and was maintained in Eagle's Minimum Essential Medium containing 1% nonessential amino acids. All media were supplemented with 10% FBS, 100 U/mL penicillin, and 100 mg/mL streptomycin. The normal human lung fibroblast (NHLF) cell line, NHLF, was obtained from TaKaRa Biomedicals. NHLF cells were propagated as monolayer culture in the medium recommended by the manufacturer. Although cell lines were not authenticated by the authors, cells were immediately expanded after receipt and stored in liquid N_2. Cells were not cultured for more than 5 months following resuscitation. The cells were maintained at 37°C in a humidified atmosphere with 5% CO_2.

Recombinant adenoviruses

The recombinant telomerase-specific replication-competent adenovirus OBP-301 (Telomelysin), in which the promoter element of the *hTERT* gene drives the expression of *E1A* and *E1B* genes, was previously constructed and characterized (12, 27). For OBP-301–mediated induction of exogenous *p53* gene expression, we recently generated OBP-702, in which a human wild-type *p53* gene expression cassette was inserted into the *E3* region (Supplementary Fig. S1; ref. 26). Ad-p53 is a replication-defective adenovirus serotype 5 vector with a *p53* gene expression cassette at the *E1* region (19, 20). Recombinant viruses were purified by ultracentrifugation using cesium chloride step gradients, their titers were determined by a plaque-forming assay using 293 cells and they were stored at −80°C.

Cell viability assay

Cells were seeded on 96-well plates at a density of 1×10^3 cells/well 24 hours before viral infection. All cell lines were infected with OBP-702 at multiplicity of infections (MOI) of 0, 0.1, 1, 10, 50, or 100 plaque-forming units (PFU)/cell. Cell viability was determined on days 1, 2, 3, and 5 after virus infection using Cell Proliferation Kit II (Roche Molecular Biochemicals). The 50% inhibiting dose (ID_{50}) value of OBP-702 for each cell line was calculated

using cell viability data obtained on day 5 after virus infection.

Time-lapse confocal laser microscopy

GFP-expressing MNNG/HOS (MNNG/HOS-GFP) cells were established by stable transfection with GFP expression plasmid using Lipofectamine LTX (Invitrogen). MNNG/HOS-GFP and NHLF cells were seeded in 35-mm glass-based dishes at a density of 1×10^5 cells/dish 24 hours before infection and were infected with OBP-702 at an MOI of 10 PFU/cell for 72 hours. Phase-contrast and fluorescence time-lapse recordings were obtained to concomitantly analyze cell morphology and GFP expression using an inverted FV10i confocal laser scanning microscopy (OLYMPUS).

Western blot analysis

SaOS-2 and MNNG/HOS cells, seeded in a 100-mm dish at a density of 1×10^5 cells/dish, were infected with OBP-301, OBP-702, or Ad-p53 at the indicated MOIs. In contrast, SaOS-2 cells were transfected with 10 nmol/L *miR-93* (Ambion), *miR-106b* (Ambion), or control miRNA (Ambion) 24 hours before Ad-p53 infection and infected with Ad-p53 at an MOI of 100 for 48 hours. Whole-cell lysates were prepared in a lysis buffer [50 mmol/L Tris-HCl (pH 7.4), 150 mmol/L NaCl, 1% Triton X-100] containing a protease inhibitor cocktail (Complete Mini; Roche) at the indicated time points. Proteins were electrophoresed on 6% to 15% SDS-PAGE and were transferred to polyvinylidene difluoride membranes (Hybond-P; GE Health Care). Blots were blocked with 5% non-fat dry milk in TBS-T (Tris-buffered saline and 0.1% Tween-20, pH 7.4). The primary antibodies used were: rabbit anti-PARP polyclonal antibody (pAb; Cell Signaling Technology), mouse anti-p53 monoclonal antibody (mAb; Calbiochem), mouse anti-$p21^{WAF1}$ mAb (Calbiochem), rabbit anti-E2F1 pAb (Santa Cruz Biotechnology), mouse anti-Ad5 E1A mAb (BD PharMingen), rabbit anti-microtubule-associated protein 1 light chain 3 (LC3) pAb [Medical & Biological Laboratories (MBL)], mouse anti-p62 mAb (MBL), rabbit anti-damage-regulated autophagy modulator (DRAM) pAb (Abgent), and mouse anti-β-actin mAb (Sigma-Aldrich).

Flow cytometric analysis

To analyze the active caspase-3 expression, cells were incubated for 20 minutes on ice in Cytofix/Cytoperm solution (BD Biosciences), labeled with phycoerythrin (PE)-conjugated rabbit anti-active caspase-3 mAb (BD Biosciences) for 30 minutes, and then analyzed using FACS array (BD Biosciences).

To evaluate the sub-G_1 population, which is a apoptosis indicator, in SaOS-2 cells after virus infection, SaOS-2 cells were seeded in a 100-mm dish at a density of 1×10^6 cells/dish 24 hours before viral infection and were infected with mock, OBP-301, Ad-p53, or OBP-702 at an MOI of 10 PFUs/cell for 48 hours. Cells were trypsinized and resuspended in original supernatant to ensure that both attached and nonattached cells were analyzed. Cells stained with propidium iodide were analyzed using FACS array (BD Biosciences).

Quantitative real-time reverse transcription PCR analysis

To evaluate the expressions of *miR-93* and *miR-106b* in tumor cells after OBP-702 infection, SaOS-2 and MNNG/HOS cells were seeded on 6-well plates at a density of 2×10^5 cells/well 24 hours before viral infection and were infected with OBP-702 at MOIs of 0, 1, 5, 10, 50, or 100 PFU/cell. Three days after virus infection, total RNA was extracted from the cells using a miRNeasy Mini Kit (Qiagen). The concentration and quality of RNA were assessed using a Nanodrop spectrophotometer. cDNA was synthesized from 10 ng of total RNA using the TaqMan MicroRNA Reverse Transcription Kit (Applied Biosystems), and quantitative real-time reverse transcription (RT)-PCR was carried out using the Applied Biosystems StepOnePlus real-time PCR System. The expressions of *miR-93* and *miR-106b* were defined from the threshold cycle (C_t), and relative expression levels were calculated using the $2^{-\Delta\Delta C_t}$ method after normalization with reference to the expression of U6 small nuclear RNA.

In vivo orthotopic MNNG/HOS xenograft tumor model

Animal experimental protocols were approved by the Ethics Review Committee for Animal Experimentation of Okayama University School of Medicine (Okayama, Japan). MNNG/HOS cells (5×10^6 cells per site) were inoculated into the tibias of female athymic nude mice aged 6 to 7 weeks (CLEA Japan). Palpable tumors developed within 21 days and were permitted to grow to approximately 5 to 6 mm in diameter. At that stage, a 50-μL volume of solution containing OBP-702, OBP-301, or Ad-p53 at a dose of 1×10^8 PFU or PBS was injected into the tumors for 3 cycles every 2 days. Tumor volume was monitored by computed tomographic (CT) imaging once a week after virus infection.

Three-dimensional computed tomography imaging

The tumor volume and formation of osteolytic lesions were evaluated using three-dimensional CT (3D-CT) imaging (ALOKA Latheta LCT-200; Hitachi Aloka Medical). The tumor volume was calculated by INTAGE Realia software (Cybernet Systems).

Histopathologic analysis

Tumors were fixed in 10% neutralized formalin and embedded in paraffin blocks. Sections were stained with hematoxylin/eosin and analyzed by light microscopy.

Statistical analysis

Data are expressed as means ± SD. Student *t* test was used to compare differences between groups. Statistical significance was defined as $P < 0.05$.

Results

In vitro cytopathic efficacy of OBP-702 against human osteosarcoma cell lines

To evaluate the *in vitro* cytopathic activity of OBP-702, we used the 2 OBP-301–sensitive human osteosarcoma cells (HOS and U2OS) and the 2 OBP-301–resistant human osteosarcoma cells (SaOS-2 and MNNG/HOS) that were recently described (14). The cell viability of each cell was assessed over 5 days after infection using the XTT assay. OBP-702 infection suppressed the viability of OBP-301–sensitive and -resistant cells in dose- and time-dependent manners (Fig. 1A and B). When the ID_{50} values of OBP-702 in all 4 human osteosarcoma cells were compared with those of OBP-301 calculated in a previous report (14), all cell lines were more sensitive to OBP-702 than to OBP-301 (Table 1). The ID_{50} values of OBP-702 were also lower than those of Ad-p53 (Supplementary Fig. S2). However, OBP-702 did not exhibit any cytopathic effect in NHLF cells (Fig. 1B). When GFP-expressing MNNG/HOS-GFP cells were cocultured with human normal NHLF cells, OBP-702 infection showed a cytopathic effect (confirmed by observation of round-shaped morphologic changes) in MNNG/HOS-GFP cells but not in NHLF cells (Fig. 1C). These results indicate that OBP-702 was more cytopathic than OBP-301 for human osteosarcoma cells but was not cytopathic for normal human cells.

Increased induction of apoptosis by OBP-702 when compared with OBP-301 or Ad-p53

We next investigated whether OBP-702 induces more profound apoptosis when compared with OBP-301 or Ad-p53. OBP-301–resistant SaOS-2 and MNNG/HOS cells

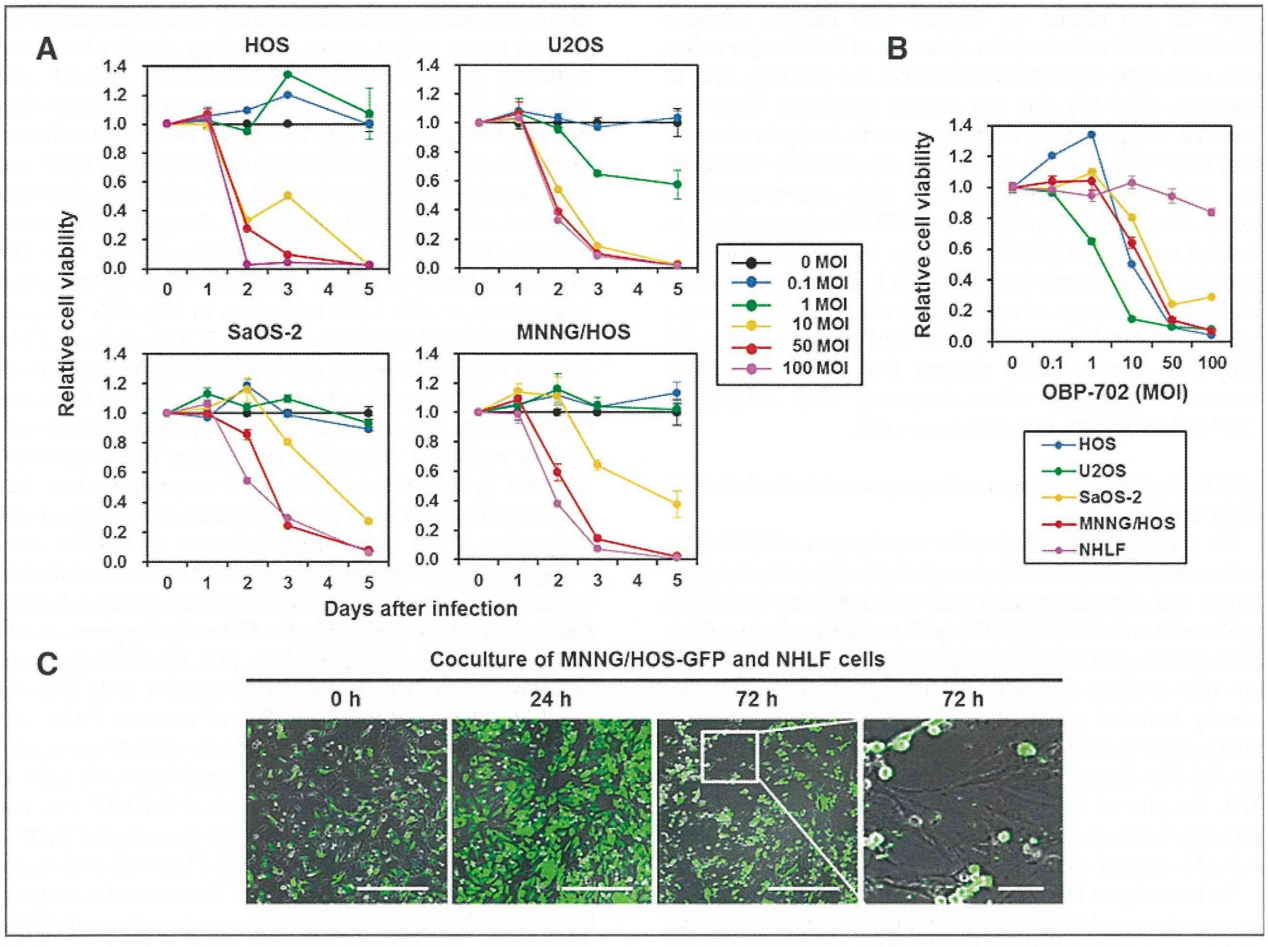

Figure 1. *In vitro* cytopathic effect of OBP-702 in human osteosarcoma cell lines. A, OBP-301–sensitive (HOS and U2OS) and OBP-301–resistant (SaOS-2 and MNNG/HOS) human osteosarcoma cells were infected with OBP-702 at the indicated MOI, and cell viability was quantified over 5 days using the XTT assay. Cell viability was calculated relative to that of the mock-infected group on each day, which was set at 1.0. Cell viability data are expressed as mean values ± SD ($n = 5$). B, four human osteosarcoma cells and one normal fibroblast NHLF cell were seeded 24 hours before viral infection and were infected with OBP-702 at the indicated MOIs, and cell viability was examined on day 5 using the XTT assay. Cell viability was calculated relative to that of the mock-infected group, which was set at 1.0. Cell viability data are expressed as mean ± SD ($n = 5$). C, time lapse images of cytopathic effect of OBP-702 in coculture of GFP-expressing MNNG/HOS cells with human normal fibroblast NHLF cells. MNNG/HOS-GFP cells coincubated with NHLF cells were recorded for 72 hours after OBP-702 infection at an MOI of 10. Three images on the left are low magnification and one image on the right is high magnification of the area outlined by a white square. Left scale bars, 100 μm. Right scale bar, 10 μm.

Table 1. Comparison of ID_{50} values of OBP-301 and OBP-702 in various human osteosarcoma cell lines

Cell lines	Sensitivity to OBP-301	Cell type	Relative hTERT mRNA expression	ID_{50} value[a] (MOI)		Ratio[b] (OBP-702/ OBP-301)
				OBP-301	OBP-702	
SaOS-2	Resistant	ALT	Negative	98.1	5.5	0.06
MNNG/HOS	Resistant	Non-ALT	1	97.3	6.7	0.07
U2OS	Sensitive	ALT	0.3	38.2	1.2	0.03
HOS	Sensitive	Non-ALT	4.3	43.0	4.5	0.10

[a]The ID_{50} values of OBP-702 and OBP-301 were calculated from the data of XTT assay on day 5 after infection.
[b]The ratio was calculated from the division of the ID_{50} value of OBP-702 by the ID_{50} value of OBP-301.

were infected with OBP-702, OBP-301, or Ad-p53, and apoptosis was assessed by Western blot and flow cytometric analyses. Western blot analysis showed that SaOS-2 cells exhibited the cleavage of PARP after infection with OBP-702 (>5 MOIs) or Ad-p53 (>50 MOIs), whereas MNNG/HOS cells had the cleavage of PARP after infection with OBP-702 (>5 MOIs) but not Ad-p53 (Fig. 2A). In contrast, OBP-301 did not induce apoptosis (data not shown). Furthermore, flow cytometric analysis showed that OBP-702 infection (10 MOIs) significantly increased the percentage of apoptotic cells with active caspase-3 when compared with Ad-p53 or OBP-301 at same doses in SaOS-2 and MNNG/HOS cells (Fig. 2B and C). Cell-cycle analysis also showed that OBP-702 (10 MOIs) induced the highest percentages of sub-G_1 population in SaOS-2 cells when compared with Ad-p53 or OBP-301 at same doses (Fig. 2D). These results suggest that OBP-702 induces increased apoptosis when compared with Ad-p53 or OBP-301 in human osteosarcoma cells.

p53 induction in human osteosarcoma cells infected with OBP-702

To investigate the molecular mechanism of OBP-702–induced apoptosis in human osteosarcoma cells, we evaluated p53 expression after OBP-702 infection in SaOS-2 (p53-null) and MNNG/HOS (p53-mutant) cells in which endogenous p53 expression level was confirmed by Western blot analysis (Supplementary Fig. S3). OBP-702 efficiently induced p53 expression in SaOS-2 and MNNG/HOS cells (Fig. 3A). The level of p53 expression was higher in OBP-702–treated cells than in Ad-p53–treated cells (Fig. 3A). Despite of OBP-702–induced high p53 expression, p53 downstream target p21 protein was induced only in Ad-p53–treated cells.

To investigate the effect of exogenous p53 overexpression in virus replication, we next compared the replication abilities of OBP-702 and OBP-301 in p53-null SaOS-2 cells by measuring the relative amounts of *E1A* copy numbers. The *E1A* copy number of OBP-702 was similar to that of OBP-301 in SaOS-2 cells (Supplementary Fig. S4). These results indicate that OBP-702 efficiently induces exogenous p53 expression without affecting p21 expression and virus replication in human osteosarcoma cells.

OBP-702–mediated upregulation of *miR-93* and *miR-106b* suppresses p21 expression

Adenoviral E1A protein has been shown to activate E2F1 expression (28), which is a multifunctional transcription factor that regulates diverse cell fates through induction of many target genes, including small noncoding miRNAs (29). Recently, E2F1-inducible *miR-93* and *miR-106b* have been shown to suppress p21 expression in human cancer cells (30). Therefore, we sought to investigate whether OBP-702 induces expressions of E2F1 and E2F1-regulated miRNAs (*miR-93* and *miR-106b*). OBP-702 infection activated E2F1 expression along with E1A accumulation in SaOS-2 and MNNG/HOS cells (Fig. 3B). The expression levels of *miR-93* and *miR-106b* were increased in association with E2F1 activation in OBP-702–infected SaOS-2 and MNNG/HOS cells (Fig. 3C). In contrast, E1A-deleted Ad-p53 infection did not increase expressions of E2F1 and E2F1-regulated *miR-93* and *miR-106b* (data not shown). Next, we assessed whether upregulation of *miR-93* and *miR-106b* efficiently suppresses p21 expression induced by Ad-p53–mediated p53 overexpression. Ad-p53 infection at MOIs of 10 and 100 efficiently induced p21 expression at 48 hours after infection in SaOS-2 cells (Supplementary Fig. S5). When SaOS-2 cells were infected with Ad-p53 at an MOI of 100 for 48 hours, pretransfection with *miR-93*, *miR-106b*, or both efficiently suppressed Ad-p53–induced p21 expression (Fig. 3D). Interestingly, both *miR-93*- and *miR-106b*–transfected SaOS-2 cells showed the 1.5-fold increased expression of cleaved PARP (C-PARP) in consistency with remarkable p21 downregulation when compared with those transfected with control miR. However, the expression level of C-PARP was not increased in the *miR-93*- or *miR-106b*–transfected SaOS-2 cells, although transfection with *miR-93* or *miR-106b* moderately decreased p21 expression. These results suggest that OBP-702 suppresses p21 expression through E1A-dependent upregulation of both E2F1-inducible *miR-93* and *miR-106b* and contributes to induction of apoptosis.

Increased induction of autophagy by OBP-702 when compared with OBP-301

Recently, we showed that oncolytic adenovirus OBP-301 mainly induces programmed cell death in association with autophagy rather than apoptosis in human tumor

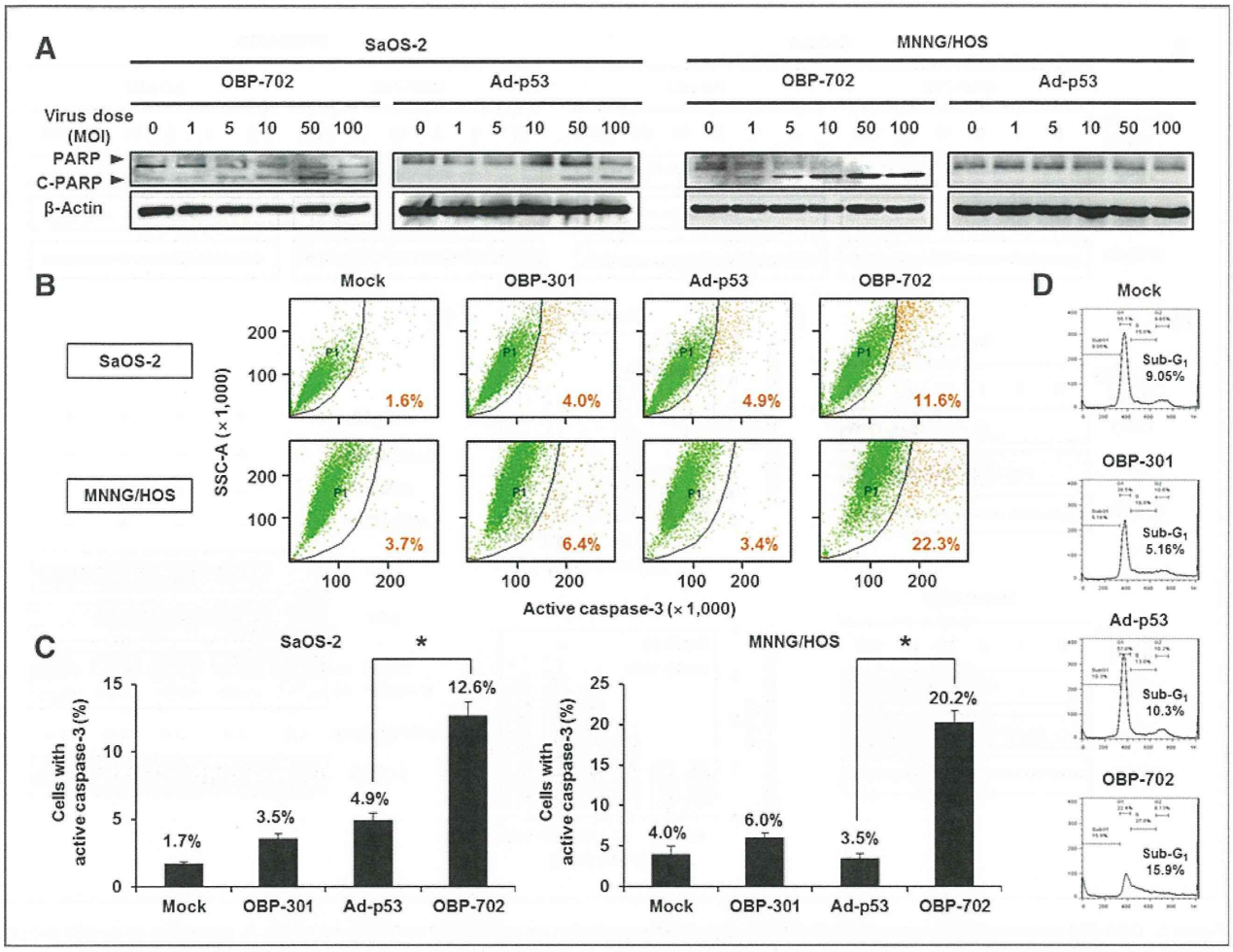

Figure 2. OBP-702 induces increased apoptosis when compared with OBP-301 or Ad-p53. A, OBP-301–resistant SaOS-2 and MNNG/HOS cells were infected with OBP-702 or Ad-p53 at the indicated MOIs for 72 hours. Cell lysates were subjected to Western blot analysis for the C-PARP and PARP. β-Actin was assayed as a loading control. B–D, SaOS-2 and MNNG/HOS cells were infected with OBP-702, OBP-301, or Ad-p53 at an MOI of 10 for 48 hours. Mock-infected cells were used as control. Caspase-3 activation was quantified using the flow cytometric analysis. Representative flow cytometric data are shown in B. The mean percentage of SaOS-2 cells and MNNG/HOS cells that express active caspase-3 was calculated on the basis of 3 independent experiments (C). The cell-cycle state was analyzed by flow cytometry in SaOS-2 cells after staining with propidium iodide. Representative cell-cycle data are shown (D). The percentage of sub-G_1 population was expressed in each graph. Bars, SD. Statistical significance was determined using Student *t* test. *, $P < 0.05$.

cells (31). Therefore, we next investigated whether OBP-702 induces more profound autophagy than does OBP-301. Western blot analysis revealed that OBP-702 infection showed increased autophagy, which was confirmed by conversion of LC3-I to LC3-II (increased ratio of LC3-II/LC3-I) and p62 downregulation, when compared with OBP-301 in MNNG/HOS cells (Fig. 4A). Moreover, the expression level of the p53-induced modulator of autophagy, DRAM (32), was decreased after OBP-301 infection, but its expression was maintained after OBP-702 infection (Fig. 4A). As p53-mediated p21 overexpression is known to inhibit both apoptosis and autophagy (17, 18), we further evaluated whether miR-mediated p21 suppression is involved in the enhancement of p53-mediated autophagy induction. Ad-p53–induced autophagy was enhanced by *miR-93*- and *miR-106b*–mediated p21 suppression (Fig. 4B). These results suggest that OBP-702 induces more profound autophagy than does OBP-301 and that this effect occurs via p53-mediated DRAM activation and miR-mediated p21 suppression.

Enhanced antitumor effect of OBP-702 in an orthotopic xenograft tumor model

Finally, to assess the *in vivo* antitumor effect of OBP-702, we used an orthotopic MNNG/HOS tumor xenograft model. OBP-702, OBP-301, Ad-p53, or PBS were intratumorally injected for 3 cycles every 2 days. OBP-702 administration significantly suppressed tumor growth when compared with OBP-301, Ad-p53, or PBS in an orthotopic MNNG/HOS tumor model (Fig. 5A and B). 3D-CT examination revealed that OBP-702–treated tumors had less bone destruction than did OBP-301- or Ad-p53–treated

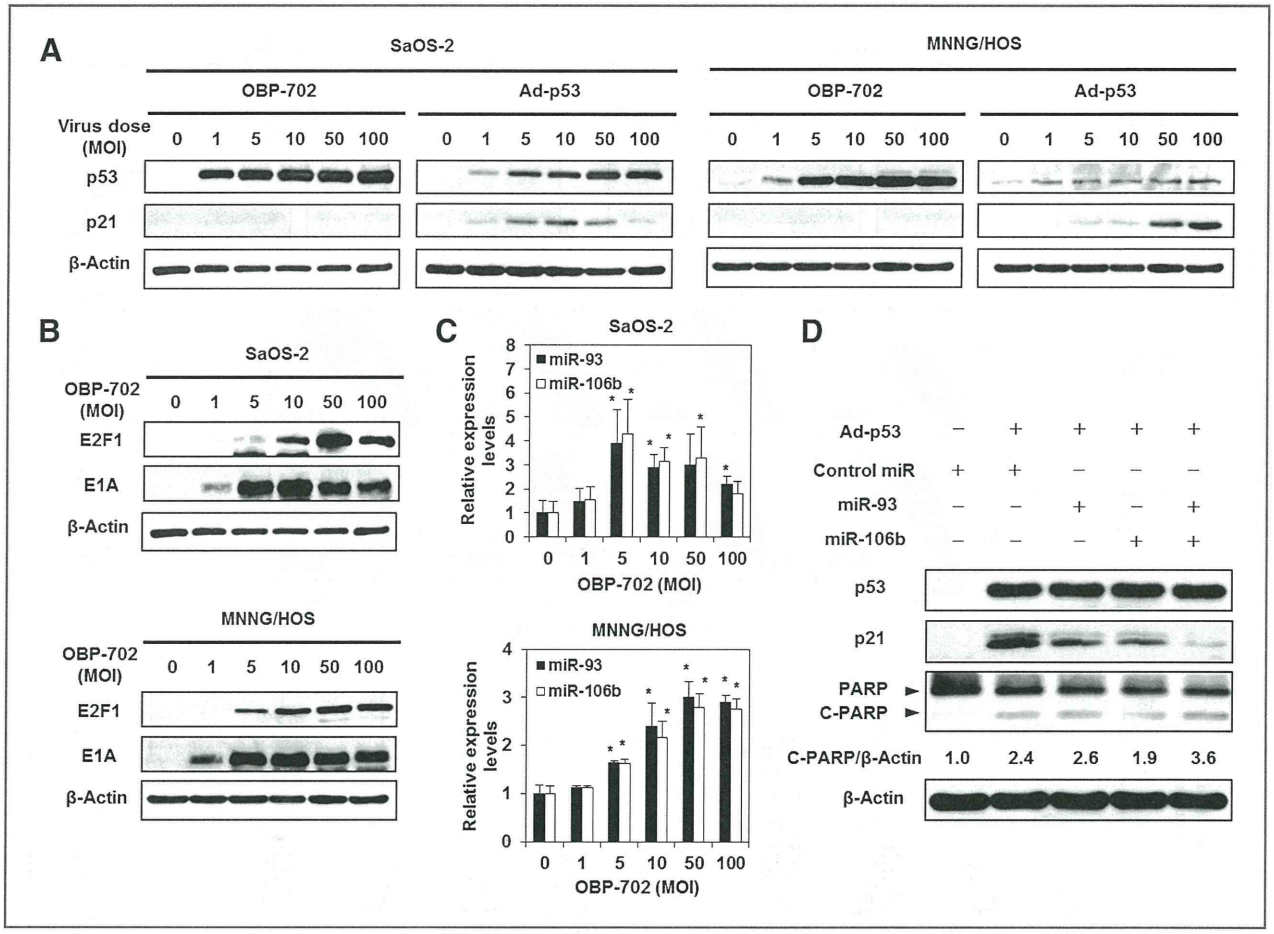

Figure 3. OBP-702 induces p53 overexpression with E1A-mediated p21 suppression via *miR-93* and *miR-106b* activation. A, expression of the p53 and p21 proteins in SaOS-2 and MNNG/HOS cells infected with OBP-702 or Ad-p53 at the indicated MOIs for 72 hours was assessed using Western blot analysis. B, expression of the E2F1 and viral E1A proteins in SaOS-2 and MNNG/HOS cells infected with OBP-702 at the indicated MOIs for 72 hours was assessed using Western blot analysis. C, expression of *miR-93* and *miR-106b* was assayed using qRT-PCR in SaOS-2 cells infected with OBP-702 at the indicated MOIs for 72 hours on 3 independent experiments. The values of *miR-93* and *miR-106b* at 0 MOI were set at 1, and the relative levels of *miR-93* and *miR-106b* at the indicated MOIs were plotted as fold induction. Bars, SD. Statistical significance was determined by Student *t* test. *, $P < 0.05$. D, SaOS-2 cells were transfected with 10 nmol/L *miR-93*, *miR-106*, or control miRNA 24 hours before Ad-p53 infection at an MOI of 100. At 48 hours after Ad-p53 infection, the expression levels of p53, p21, PARP, and C-PARP were examined by Western blot analysis. β-Actin was assayed as a loading control. By using ImageJ software, the expression level of C-PARP protein was calculated relative to its expression in the control miR–treated cells, whose expression level was designated as 1.0.

tumors (Fig. 5C). On histopathologic analysis, there were large necrotic areas in OBP-702–treated tumors but not in OBP-301- or Ad-p53–treated tumors (Fig. 5D). Moreover, the expression of the cell proliferation marker, Ki67, was also decreased, especially in OBP-702–treated tumor cells (Supplementary Fig. S6). These results suggest that OBP-702 eliminates tumor tissues more efficiently when compared with OBP-301 or Ad-p53.

Discussion

We previously reported that telomerase-specific replication-competent oncolytic adenovirus OBP-301 has strong antitumor activity in a variety of human epithelial and nonepithelial malignant cells (12, 14, 27). However, some human osteosarcoma cells were resistant to the cytopathic activity of OBP-301 (14). In this study, we showed that a novel p53-expressing oncolytic adenovirus, OBP-702, had increased *in vitro* and *in vivo* antitumor effects than did OBP-301 in human osteosarcoma cells (Fig. 1 and 5). OBP-702 induced increased apoptosis in association with p53 upregulation and p21 downregulation when compared with replication-deficient Ad-p53 (Fig. 2 and 3A). E1A-dependent upregulation of *miR-93* and *miR-106b* was involved in OBP-702–mediated suppression of p21 expression (Fig. 3). Moreover, p53-mediated DRAM activation with p21 suppression enhanced oncolytic adenovirus-mediated autophagy induction (Fig. 4). Recent studies suggest that transgene-expressing armed oncolytic adenoviruses are a promising antitumor strategy for induction of oncolytic and transgene-induced cell death (33). Although p53 overexpression has been shown to enhance antitumor

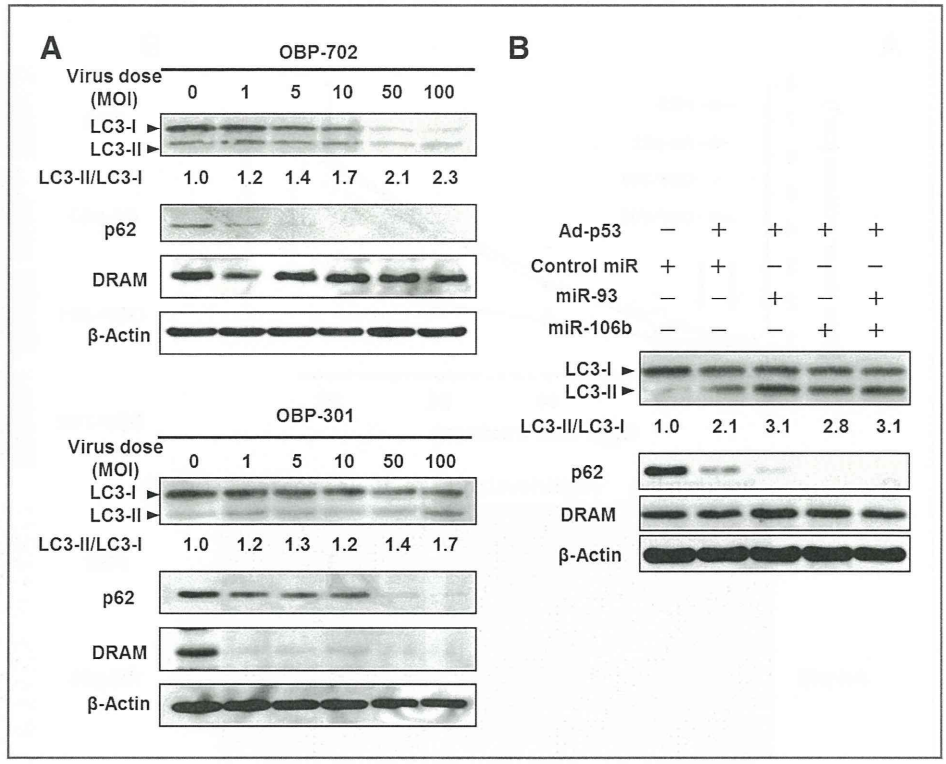

Figure 4. OBP-702 induces increased autophagy when compared with OBP-301. A, MNNG/HOS cells were infected with OBP-702 or OBP-301 at the indicated MOIs for 72 hours. Cell lysates were subjected to Western blot analysis for LC3, p62, and DRAM. B, SaOS-2 cells were transfected with 10 nmol/L *miR-93*, *miR-106*, or control miRNA 24 hours before Ad-p53 infection. At 48 hours after Ad-p53 infection at an MOI of 100, the expression levels of LC3, p62, and DRAM were examined by Western blot analysis. β-Actin was assayed as a loading control. By using ImageJ software, the ratio of LC3-II/LC3-I expressions was calculated relative to its expression in the mock-infected cells, whose expression level was designated as 1.0.

activity of oncolytic adenoviruses (34), the molecular mechanisms by which p53 mediates enhancement of the antitumor effect remain unclear. Recently, we reported that OBP-702 induces profound apoptosis through p53-dependent BAX upregulation and E1A-dependent p21 and MDM2 downregulation in epithelial malignant cells (26). Thus, oncolytic adenovirus-mediated p53 overexpression likely induces dual apoptotic and autophagic cell death pathways through p53-dependent BAX/DRAM activation and E1A-dependent p21/MDM2 suppression with E2F1-inducible *miR-93/106b* upregulation (Fig. 6).

OBP-702 efficiently suppressed the cell viability of both OBP-301–sensitive and -resistant osteosarcoma cells (Fig. 1). We previously reported that OBP-301–resistant SaOS-2 cells have no *hTERT* mRNA expression (Table 1), suggesting that SaOS-2 cells maintain telomere length through alternative lengthening of telomeres (ALT). As *hTERT* gene promoter is used for tumor-specific replication of OBP-301, ALT-type human osteosarcoma cells such as SaOS-2 cells may be resistant to OBP-301. However, ALT-type SaOS-2 cells showed similar sensitivity to OBP-702 as well as non–ALT-type MNNG/HOS cells (Fig. 1 and Table 1). These results suggest that p53 overexpression overcomes resistance to OBP-301 in ALT-type SaOS-2 cells. As the replication rate of OBP-702 was almost similar that of OBP-301 in ALT-type SaOS-2 cells (Supplementary Fig. S2), p53-induced cell death pathway would suppress the cell viability of ALT-type human osteosarcoma cells.

OBP-702–mediated p53 overexpression induced 2 types of programmed cell deaths (i.e., apoptosis and autophagy), thereby contributing to the enhancement of the antitumor effect of OBP-301 in human osteosarcoma cells (Fig. 2 and 4). As p53 downstream target p21 functions as a suppressor of apoptosis and autophagy (17, 18), p21 suppression may be a critical factor to induce dual programmed cell death pathways in response p53 overexpression. Suppression of p21 expression by genetic deletion or artificial p21 target microRNA has been shown to enhance the Ad-p53–induced apoptosis (18, 35). Inactivation of p21 by adenoviral E1A has been shown to enhance apoptosis in chemotherapeutic drug-treated human colon cancer cells that overexpress p53 (36). Genetic deletion of p21 has been also shown to induce autophagy in mouse embryonic fibroblasts treated with C (2)-ceramide or γ-irradiation (17). In contrast, p21 overexpression inhibited the Ad-p53–mediated apoptosis induction (18). Thus, E1A-mediated p21 downregulation would enhance p53-induced apoptosis and autophagy in OBP-702–infected cells.

E1A-dependent E2F1 activation and subsequent upregulation of E2F1-inducible miRNAs efficiently suppressed p21 expression, leading to the enhancement of p53-induced apoptosis and autophagy, in OBP-702–infected osteosarcoma cells (Figs. 2–4). Recent studies suggest that the cross-talk between p53 and E2F1 play a role in the regulation of diverse cell fates (37). For example, co-expression of p53 and E2F1 contributes to induction of apoptosis (38, 39). We previously showed